

Phase separation under two-dimensional Poiseuille flow

Hirohito Kiwata

Division of Natural Science, Osaka Kyoiku University, Kashiwara, Osaka 582-8582, Japan

(Received 25 September 2000; revised manuscript received 4 December 2000; published 12 April 2001)

The spinodal decomposition of a two-dimensional binary fluid under Poiseuille flow is studied by numerical simulation. We investigated time dependence of domain sizes in directions parallel and perpendicular to the flow. In an effective region of the flow, the power-law growth of a characteristic length in the direction parallel to the flow changes from the diffusive regime with the growth exponent $\alpha = \frac{1}{3}$ to a new regime. The scaling invariance of the growth in the perpendicular direction is destroyed after the diffusive regime. A recurrent prevalence of thick and thin domains which determines log-time periodic oscillations has not been observed in our model. The growth exponents in the infinite system under two-dimensional Poiseuille flow are obtained by the renormalization group.

DOI: 10.1103/PhysRevE.63.051505

PACS number(s): 64.75.+g, 47.20.-k

I. INTRODUCTION

When an immiscible binary fluid is quenched into an unstable two-phase region, phase separation occurs. The time dependence of phase separation has attracted much attention for several decades. The most prominent result for the phase separation is that the average domain size is characterized by the growth law

$$R(t) \sim t^\alpha, \quad (1)$$

where α is a growth exponent. The growth exponent α takes different values depending on the mechanism controlling the growth of domains. In the so-called diffusive regime, the growth exponent becomes $\alpha = \frac{1}{3}$ irrespective of the spatial dimension [1].

The phase separation under the shear flow has not only been technologically important, but also extensively studied from purely scientific points of view in recent years [2]. It has been reported that the shear flow alleviates frustration of the system and speeds up the system reaching the stable state [3,4]. In the present paper, we study the phase separation of a two-dimensional binary fluid under the Poiseuille flow. We solve a time-dependent Ginzburg-Landau equation numerically and examine the power-law growth of the average domain size in the direction parallel and perpendicular to the flow. Our calculations are focused on two points. First, the phase separation under the Poiseuille flow is modified from those under the shear flow. In the case of the shear flow, the distance dependence of the flow is linear, but in the case of the Poiseuille flow it is quadratic. One can suppose that the power-law dependence of the domain size under the Poiseuille flow is quite different from those under the shear flow. Under the shear flow the power-law dependences of the domain size in the diffusive regime are given by

$$R_{\parallel}(t) \sim t^{4/3} \quad \text{and} \quad R_{\perp}(t) \sim t^{1/3}, \quad (2)$$

where R_{\parallel} and R_{\perp} are the average domain sizes in the direction parallel and perpendicular to the shear flow, respectively [5]. Although the growth exponent of the domain size in the direction perpendicular to the shear flow remains the same as those without the flow, the exponent in the direction parallel

to the flow increases from $\frac{1}{3}$ to $\frac{4}{3}$. When the dimension of the order parameter becomes infinity, the situation is similar. In this case the growth exponents have been calculated as $\alpha = \frac{5}{4}$ and $\alpha = \frac{1}{4}$, disregarding the log correction, in the direction parallel and perpendicular to the shear flow, respectively [6–8], and the growth exponent without flow is given by $\alpha = \frac{1}{4}$ [9]. The shear flow enhances the domain growth in the direction parallel to the flow. Under Poiseuille flow the similar enhancement of the domain size is expected. Second, it is interesting to investigate effects of flow in confined geometry. The dynamics of the phase separation in the presence of walls without the flow have been reported by several authors [10–13]. These authors studied the growth of the wetting layers, and showed that although the average domain size differs in magnitude, the growth exponent in both the direction parallel and perpendicular to the walls are the same. In the present paper, the two-dimensional Poiseuille flow is defined between two static plates.

The outline of the present paper is as follows: In Sec. II, we introduce the model and the numerical method used in the integration of the equation. The rigid-wall conditions are also presented in this section. In Sec. III, we show the results for the time dependence of the average domain sizes. Section IV gives summary and discussion.

II. MODEL AND NUMERICAL METHOD

We start from the Ginzburg-Landau expression of the free energy functional $F\{\phi\}$,

$$F\{\phi\} = \int \int_{\Omega} dx dy \frac{1}{2} \left[-\frac{1}{2} \phi^2 + \frac{1}{4} \phi^4 + \frac{1}{2} (\nabla \phi)^2 \right], \quad (3)$$

where ϕ is the difference of the local concentration of the two components of a mixture. Let the region be $\Omega = \{(x, y) | 0 \leq x \leq L, 0 \leq y \leq L\}$. We define the system confined between two parallel plates at $y=0$ and $y=L$. The time dependence of the field variable ϕ without the flow is given by the following Langevin equation:

$$\frac{\partial \phi}{\partial t} = \nabla^2 \frac{\delta F}{\delta \phi}, \quad (4)$$

where we disregard the noise term, which has been shown an irrelevant variable by renormalization group [1,14,15]. In order to conserve the sum of the field variable, we examine the boundary conditions in detail. The sum of the field variable is defined by

$$I = \int \int_{\Omega} dx dy \phi. \quad (5)$$

Under the conservation conditions, the value (5) is independent of time

$$\begin{aligned} \frac{dI}{dt} &= \int \int_{\Omega} dx dy \frac{\partial \phi}{\partial t} \\ &= \int \int_{\Omega} dx dy \frac{1}{2} \left(\frac{\partial^2}{\partial x^2} + \frac{\partial^2}{\partial y^2} \right) \\ &\quad \times \left[-\phi + \phi^3 - \left(\frac{\partial^2}{\partial x^2} + \frac{\partial^2}{\partial y^2} \right) \phi \right] = 0. \end{aligned} \quad (6)$$

Deriving the second line from the first line, we used the time differential equation (4). The boundary conditions which set Eq. (6) to zero are

$$\left. \frac{\partial \phi(x,y,t)}{\partial x} \right|_{x=0} = \left. \frac{\partial \phi(x,y,t)}{\partial x} \right|_{x=L}, \quad (7)$$

$$\left. \frac{\partial^3 \phi(x,y,t)}{\partial x^3} \right|_{x=0} = \left. \frac{\partial^3 \phi(x,y,t)}{\partial x^3} \right|_{x=L}, \quad (8)$$

$$\left. \frac{\partial \phi(x,y,t)}{\partial y} \right|_{y=0} = 0, \quad \left. \frac{\partial \phi(x,y,t)}{\partial y} \right|_{y=L} = 0, \quad (9)$$

$$\left. \frac{\partial^3 \phi(x,y,t)}{\partial y^3} \right|_{y=0} = 0, \quad \left. \frac{\partial^3 \phi(x,y,t)}{\partial y^3} \right|_{y=L} = 0. \quad (10)$$

Henceforth we impose the periodic boundary conditions at $x=0$ and $x=L$ and the rigid-wall boundary conditions at $y=0$ and $y=L$. If $\phi(x+L,y,t) = \phi(x,y,t)$, Eqs. (7) and (8) are automatically satisfied. Equations (9) and (10) at $y=0$ and $y=L$ are the rigid-wall conditions. These conditions guarantee no flux through the rigid wall at $y=0$ and $y=L$. Here, we do not take account of any interaction potential between the rigid wall and the binary fluid.

In order to solve the differential equation (4), we adopt a finite-difference approximation for both the spatial and temporal derivatives [16]. In this approximation the following definitions are used:

$$x_i = i \Delta x, \quad y_j = j \Delta y, \quad t_n = n \Delta t, \quad (11)$$

$$\phi(i,j,n) = \phi(x_i, y_j, t_n). \quad (12)$$

We consider a $N \times N$ lattice with $N=256$. The values of i and j are ranging from 0 to $N-1$. The rigid-wall boundary conditions are also rewritten in the finite-difference form

$$\left. \frac{\partial \phi(x,y,t)}{\partial y} \right|_{y=0} = 0 \Rightarrow \phi(i,-1,n) - \phi(i,0,n) = 0, \quad (13)$$

$$\begin{aligned} \left. \frac{\partial^3 \phi(x,y,t)}{\partial y^3} \right|_{y=0} &= 0 \\ &\Rightarrow \phi(i,-2,n) - 3\phi(i,-1,n) + 3\phi(i,0,n) \\ &\quad - \phi(i,1,n) = 0. \end{aligned} \quad (14)$$

From Eqs. (13) and (14), one easily obtains

$$\phi(i,-2,n) = \phi(i,1,n), \quad \phi(i,-1,n) = \phi(i,0,n). \quad (15)$$

One can also get similar equations at $y=L$,

$$\phi(i,N+1,n) = \phi(i,N-2,n), \quad \phi(i,N,n) = \phi(i,N-1,n). \quad (16)$$

Under externally applied flow the following dynamical equation after quench replaces the Eq. (4)

$$\frac{\partial \phi}{\partial t} + \vec{v} \cdot \vec{\nabla} \phi = \nabla^2 \frac{\delta F}{\delta \phi}, \quad (17)$$

where the term $\vec{v} \cdot \vec{\nabla} \phi$ represents the effect of convection by the hydrodynamic flow. \vec{v} is equal to the externally imposed velocity field. For two-dimensional Poiseuille flow, $\vec{v} = (v_x, v_y)$ is given by $(v_x, v_y) = (-V_0(2/L)^2 y(y-L), 0)$ [17]. In our simulations we used the maximum of the velocity $V_0=0.01$. Our model is justified on the assumption that the two components of the binary liquid have similar mechanical properties and the external flow is not a rapid stream. The boundary conditions discussed above have not been altered by the external flows. In the finite-difference form, we used the center-difference scheme. Therefore, the convection term becomes

$$v_x(y) \frac{\partial \phi}{\partial x} \Rightarrow v_x(j) \frac{\phi(i+1,j,n) - \phi(i-1,j,n)}{2\Delta x}. \quad (18)$$

We investigated the dynamics of the phase separation in the discrete model for a critical quench. The values of the field ϕ were initially distributed as random numbers between $[-0.1, 0.1]$ under the condition that the sum of the field variable at each lattice points equals zero. We practiced eight runs at each initial random distribution. The average of all initial configuration corresponds to the average over the thermal noise. In our simulations we used a time step $\Delta t=0.3$ and spatial mesh sizes $\Delta x = \Delta y = 1.7$ [16]. Our simulations with these choice of the time step and spatial mesh sizes did not suffer from numerical instabilities at least up to the maximum of the time $n_{\max}=600\,000$.

III. RESULTS

In this section we discuss the results of the numerical simulations. In Fig. 1 we show a sequence of configurations of the field ϕ . The top and bottom lines denote rigid walls.

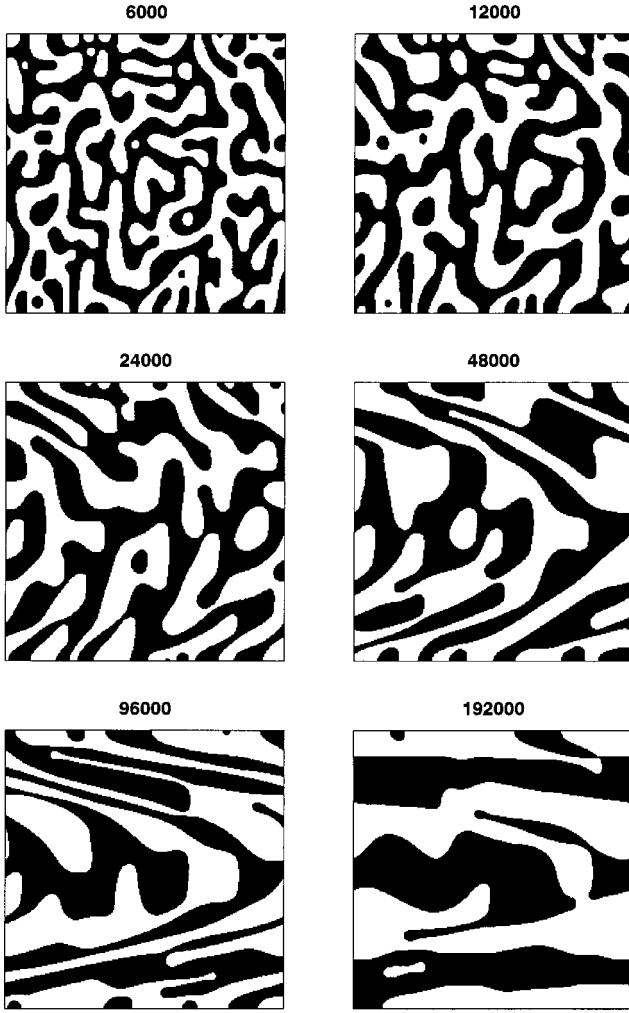


FIG. 1. A sequence of configurations of the field ϕ at time $t = 6000, 12\,000, 24\,000, 48\,000, 96\,000, 192\,000$.

After the early stage, domains are forming from the mixed initial state and a bicontinuous structure is observed. The influence of the external flow is recognized in the snapshots after $t = 24\,000$. The domains have been extended along the flow.

In order to analyze the domain growth quantitatively, we define the pair correlation function. Since the system is not isotropic, the pair correlation function is defined each in the direction parallel and perpendicular to the flow separately. The pair correlation function g_x along the flow is defined as

$$g_x(k, n) = \frac{1}{N} \sum_{j=0}^{N-1} \left\langle \frac{1}{N} \sum_{i=0}^{N-1} \phi(i+k, j, n) \phi(i, j, n) \right\rangle, \quad (19)$$

where the angular bracket denotes an average over all runs. Since the system under two-dimensional Poiseuille flow is symmetric with respect to the $j = (N-1)/2$ line, we define the pair correlation function in each region $0 \leq j \leq N/2 - 1$ and $N/2 \leq j \leq N - 1$ and average them as follows:

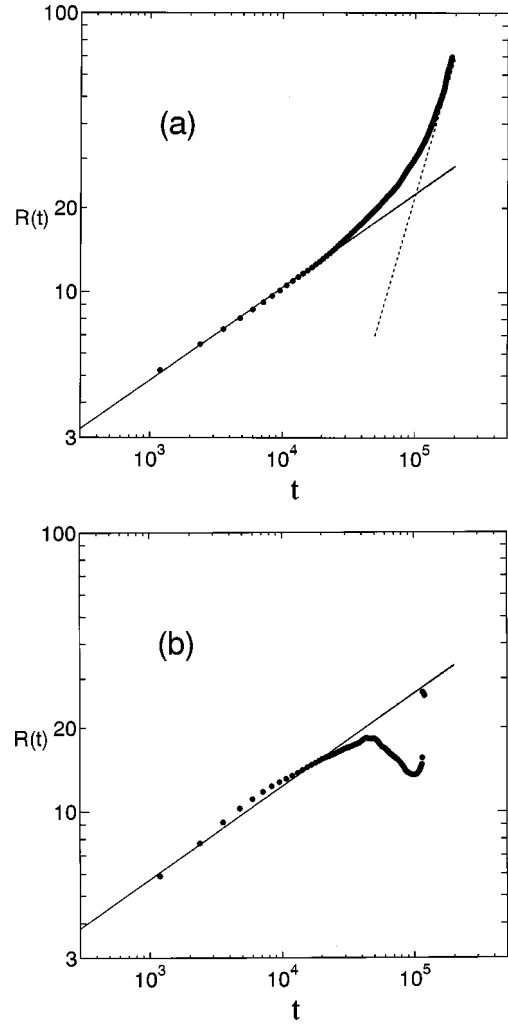


FIG. 2. (a) Time evolution of R_{\parallel} . The solid and dotted line denote the $t^{1/3}$ and $t^{5/3}$ power-law growth, respectively. (b) Time evolution of R_{\perp} . The solid line denotes the $t^{1/3}$ power-law growth.

$$g_y(k, n) = \frac{1}{N} \sum_{i=0}^{N-1} \left\langle \frac{1}{\frac{N}{2}-k} \sum_{j=0}^{N/2-1-k} \phi(i, j+k, n) \phi(i, j, n) \right\rangle + \frac{1}{N} \sum_{i=0}^{N-1} \left\langle \frac{1}{\frac{N}{2}-k} \sum_{j=N/2}^{N-1-k} \phi(i, j+k, n) \phi(i, j, n) \right\rangle, \quad (20)$$

where the denominator in the angular bracket comes from the result that the number of a pair of $\phi(i, j+k, n)$ and $\phi(i, j, n)$ is $N/2 - k$ in the regions $0 \leq j \leq N/2 - 1$ or $N/2 \leq j \leq N - 1$. We confirmed the validity of this definition (20) by means of comparing the results from Eq. (19) with those from Eq. (20) for no flow system. The locations of the first zeros of these functions (19) and (20) are taken as measures of the characteristic length $R_{\parallel}(t)$ and $R_{\perp}(t)$ in the direction parallel and perpendicular to the flow, respectively.

In Fig. 2 we show log-log plots of the characteristic length $R_{\parallel}(t)$ and $R_{\perp}(t)$ vs time t . The oscillating behavior of

$R_{\parallel}(t)$ and $R_{\perp}(t)$ in the shear flow case could not be observed. The solid lines in Figs. 2(a) and 2(b) show the power law $t^{1/3}$. In the beginning both of $R_{\parallel}(t)$ and $R_{\perp}(t)$ grow with the exponent $\alpha = \frac{1}{3}$. After this stage the behavior of $R_{\parallel}(t)$ are quite different from that of $R_{\perp}(t)$. The growth of $R_{\parallel}(t)$ is enhanced due to the flow. After passing through a transitional stage the curve approaches to a line with a constant slope. This result indicates the existence of a new regime with power-law growth. In the case of $R_{\perp}(t)$, on the other hand, after the diffusive regime it saturates and decreases with time. The decrease of $R_{\perp}(t)$ has been caused by breakup of domains by the external flow. In this time region the numerical simulation with a different initial configuration has a different form of g_y . We conclude that the scaling invariance in the direction perpendicular to the flow is broken by the flow.

In order to analyze the power-law growth under the influence of the external flow, we estimate the growth exponents by the renormalization group method [5]. We start from the following Langevin equation:

$$\frac{\partial \phi}{\partial t} + \vec{v} \cdot \vec{\nabla} \phi = \Gamma \nabla^2 \frac{\delta F}{\delta \phi} + \eta, \quad (21)$$

where a transport coefficient Γ and the thermal noise η have been reinstated explicitly. The mean value of η is zero and η satisfies the relation

$$\langle \eta(\vec{r}_1, t_1) \eta(\vec{r}_2, t_2) \rangle = -2T\Gamma \nabla^2 \delta(\vec{r}_1 - \vec{r}_2) \delta(t_1 - t_2), \quad (22)$$

where T is the temperature of the binary fluid and the angular brackets denote ensemble average. For simplicity, let the velocity be $\vec{v} = \gamma y^2 \vec{e}_x$. We introduce the fourier components of the field ϕ by $\phi_{\vec{k}}(t) = V^{-1/2} \int d\vec{r} \phi(\vec{r}, t) \exp(i\vec{k} \cdot \vec{r})$. In the \vec{k} space, the Langevin equation (21) becomes

$$\frac{\partial \phi_{\vec{k}}(t)}{\partial t} + i\gamma k_x \frac{\partial^2 \phi_{\vec{k}}(t)}{\partial k_y^2} = -\Gamma k^2 \frac{\delta F}{\delta \phi_{-\vec{k}}(t)} + \eta_{\vec{k}}, \quad (23)$$

with

$$\langle \eta_{\vec{k}}(t_1) \eta_{-\vec{k}}(t_2) \rangle = 2\vec{k}^2 T \Gamma \delta(t_1 - t_2). \quad (24)$$

The renormalization group consists of the change of the scale and the renormalization of the field

$$k'_x = k_x b^{\alpha_x}, \quad k'_y = k_y b^{\alpha_y}, \quad t' = t b^{-1}, \quad (25)$$

$$\phi_{\vec{k}}(t) = b^{\zeta} \phi'_{\vec{k}}(t'), \quad (26)$$

where b is the dilatation factor. The existence of the characteristic length implies that the structure factor has the scaling form

$$S(\vec{k}, t) = \langle \phi_{\vec{k}}(t) \phi_{-\vec{k}}(t) \rangle = R_{\parallel}(t) R_{\perp}(t) f(x, y), \quad (27)$$

where $x = k_x R_{\parallel}(t)$ and $y = k_y R_{\perp}(t)$. In order that the above equation (27) is invariant under the scale transformations (25) and (26), the relation $2\zeta = \alpha_x + \alpha_y$ is obtained. The in-

variance of the variable x and y under the scale transformations implies that α_x and α_y correspond to the growth exponents in the direction parallel and perpendicular to the flow, respectively. We assume that the fixed point free energy satisfies the relation

$$F\{b^{\zeta} \phi'_{\vec{k}}(t')\} = b^{\alpha_x} F\{\phi'_{\vec{k}}(t')\}. \quad (28)$$

This relation stems from the result that the main contribution to the free energy is due to the interfaces along the flow. By substituting Eqs. (25) and (26) into the Langevin equation (23) and relation (24) with Eq. (28), one obtains a Langevin equation with transformed parameters

$$\Gamma' = \Gamma b^{\alpha_x - 2\alpha_y - 2\zeta + 1}, \quad \gamma' = \gamma b^{-\alpha_x + 2\alpha_y + 1}, \quad T' = T b^{-\alpha_x}, \quad (29)$$

where we used the relation $k_x \ll k_y$ and disregarded k_x in \vec{k}^2 . The relation $k_x \ll k_y$ is satisfied at late time. The above recursion relations (29) are the same as ones under the shear flow except γ' [5]. A fixed point of Eq. (29) is obtained when $\alpha_x = \frac{5}{3}$ and $\alpha_y = \frac{1}{3}$. It has been shown that the temperature is the irrelevant variable.

Taking account of the result from the renormalization group, we reconsider the result of the numerical simulations. The growth exponent of $R_{\parallel}(t)$ is expected to approach $\alpha = \frac{5}{3}$. The dotted line in Fig. 2(a) denotes the power-law growth with $\alpha = \frac{5}{3}$. In the direction perpendicular to the flow the growth exponent $\alpha = \frac{1}{3}$ is obtained by the renormalization group. However, the boundary condition has not been taken account of in the renormalization group method. The breakdown of the scale invariance in the direction perpendicular to the flow originates from the rigid-wall boundary conditions. These boundary effects are observed in a sequence of the configuration of the field variable ϕ at different times. Since the velocity field on the rigid walls is zero, domains near the rigid walls have been nearly still. On the other hand, the velocity field at the center of two plates is high, so that domains have been drifting quickly. Domains repeat breakup and adhesion, and these cause the breakdown of the scale invariance in the direction perpendicular to the flow.

IV. SUMMARY AND DISCUSSION

We investigate the phase separation of binary fluid under the two-dimensional Poiseuille flow by the numerical simulations. The time dependence of the average domain size is examined. At an early stage the characteristic length in the direction parallel and perpendicular to the flow have the growth exponent in the diffusive regime $\alpha = \frac{1}{3}$. At a late stage, the time dependence of $R_{\parallel}(t)$ is quite different from that of $R_{\perp}(t)$. After a transitional stage the growth exponent of the average domain size along the flow is given by $\alpha = \frac{5}{3}$. The effect of the flow enhances the growth in the direction parallel to the flow. In the case of $R_{\perp}(t)$, after the diffusive regime we observed the breakdown of the scale invariance. The breakdown of the scale invariance is caused by repetitions of breakup and adhesion of domains. The breakup and adhesion of domains result from the velocity

field which varies from place to place in the direction perpendicular to the flow.

We estimated the growth exponents by the renormalization group method. The growth exponents $\alpha = \frac{5}{3}$ and $\alpha = \frac{1}{3}$ in the direction parallel and perpendicular to the flow are obtained, respectively. The system to which we applied the renormalization group is defined in the infinite system, so that the boundary effects are disregarded. It is impossible to impose the periodic boundary condition on the system under the two-dimensional Poiseuille flow in the direction perpendicular to the flow.

Finally, we compare the present Poiseuille flow case with the shear flow case [5]. In the shear flow case, the recurrent prevalence of thick and thin domains causes the log-time periodic oscillations of the average domain sizes. The oscil-

latory behavior of the average domain sizes prevents a straightforward computation of the growth exponents. In the case of the two-dimensional Poiseuille flow, the log-time periodic oscillations of the characteristic length have not been observed. Because of the breakdown of the scaling invariance in the direction perpendicular to the flow, our model have not been suffered from the competition between the characteristic lengths. As a result the growth exponent along the flow is obtained by the numerical simulations.

ACKNOWLEDGMENT

We thank Professor T. Inagaki for a critical reading of the manuscript and encouragement.

-
- [1] A. J. Bray, *Adv. Phys.* **43**, 357 (1994).
 - [2] A. Onuki, *J. Phys.: Condens. Matter* **9**, 6119 (1997).
 - [3] G. Gonnella, E. Orlandini, and J. M. Yeomans, *Phys. Rev. Lett.* **78**, 1695 (1997).
 - [4] A. V. Zvelindovsky, G. J. A. Sevink, B. A. C. van Vlimmeren, N. M. Maurits, and J. G. E. M. Fraaije, *Phys. Rev. E* **57**, R4879 (1998).
 - [5] F. Corberi, G. Gonnella, and A. Lamura, *Phys. Rev. Lett.* **83**, 4057 (1999).
 - [6] N. P. Rapapa and A. J. Bray, *Phys. Rev. Lett.* **83**, 3856 (1999).
 - [7] F. Corberi, G. Gonnella, and A. Lamura, *Phys. Rev. Lett.* **81**, 3852 (1997).
 - [8] F. Corberi, G. Gonnella, and A. Lamura, *Phys. Rev. E* **61**, 6621 (2000).
 - [9] A. Coniglio and M. Zannetti, *Europhys. Lett.* **10**, 575 (1989).
 - [10] R. Toral and A. Chakrabarti, *Phys. Rev. B* **43**, 3438 (1991).
 - [11] G. Brown and A. Chakrabarti, *Phys. Rev. A* **46**, 4829 (1992).
 - [12] J. F. Marko, *Phys. Rev. E* **48**, 2861 (1993).
 - [13] H. Chen and A. Chakrabarti, *Phys. Rev. E* **55**, 5680 (1997).
 - [14] A. J. Bray, *Phys. Rev. Lett.* **62**, 2841 (1989).
 - [15] A. J. Bray, *Phys. Rev. B* **41**, 6724 (1990).
 - [16] T. M. Rogers, K. R. Elder, and R. C. Desai, *Phys. Rev. B* **37**, 9638 (1988).
 - [17] L. D. Landau and E. M. Lifshitz, *Fluid Mechanics* (Pergamon Press, Oxford, 1987).